Dissertations and Theses

5-2019

Optimal Battery Weight Fraction for Serial Hybrid Propulsion System in Aircraft Design

Tsz Him Yeung

Follow this and additional works at: https://commons.erau.edu/edt

Part of the Propulsion and Power Commons

OPTIMAL BATTERY WEIGHT FRACTION FOR

SERIAL HYBRID PROPULSION SYSTEM IN AIRCRAFT DESIGN

A Thesis

Submitted to the Faculty

of

Embry-Riddle Aeronautical University

by

Tsz Him Yeung

In Partial Fulfillment of the

Requirements for the Degree

of

Master of Science in Aerospace Engineering

May 2019

Embry-Riddle Aeronautical University

Daytona Beach, Florida

OPTIMAL BATTERY WEIGHT FRACTION FOR
SERIAL HYBRID PROPULSION SYSTEM IN AIRCRAFT DESIGN

by

Tsz Him Yeung

A Thesis prepared under the direction of the candidate's committee chairman, Dr.
Richard P. Anderson, Department of Aerospace Engineering, and has been approved by
the members of the thesis committee. It was submitted to the School of Graduate Studies
and Research and was accepted in partial fulfillment of the requirements for the degree of
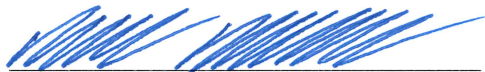Master of Science in Aerospace Engineering.

THESIS COMMITTEE

_____
Chairman, Dr. Richard P. Anderson

_____
Member, Dr. Steven Daniel
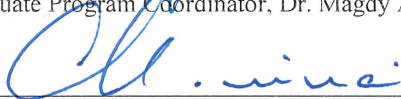
_____
Member, Dr. Mark Ricklick

_____   4.23.2019
Graduate Program Coordinator, Dr. Magdy Attia   Date
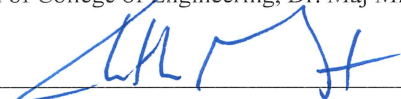
_____   4/24/19
Dean of College of Engineering, Dr. Maj Mirmirani   Date

_____   4/24/19
Senior Vice President for Academic Affairs and Provos, Dr. Lon Moeller   Date

TABLE OF CONTENTS

LIST OF TABLES

LIST OF FIGURES

SYMBOLS

b	Battery
C_{batt}	Cost of electricity per unit energy
C_{gas}	Cost of gas per unit energy
C_{max}	Maximum C-rate draw
D	Drag
E	Energy
g	Gravitational Constant
K_{batt}	Carbon emissions due to charging battery per unit energy
K_{gas}	Carbon emissions due to consuming gasoline per unit energy
L	Lift
N_p	Number of cells in parallel
N_s	Number of cells in series
P	Power
p	Propeller
Q	Capacitance
R	Range
t	Time/ Endurance
V	Velocity
V_x	Voltage
W	Weight
W_c	Battery pack knock down factor
x	Percent Hybrid
α	Charging Fuel Weight Fraction
β	Energy Weight Fraction
η	Efficiency
ρ	Specific Energy

ABBREVIATIONS

Avg	Average
ANL	Argonne National Laboratory
Ch	Charge
CO_2e	Carbon Dioxide Equivalent
Cr	Cruise
DOC	Direction Operating Cost
EFRC	Eagle Flight Research Center
EM	Electric Motor
Eng	Engine
Gas	Gasoline
Gen	Generator
GHG	Green House Gas
GREET	Greenhouse gases, Regulated Emissions, and Energy use in Transportation
LFP	Lithium Iron Phosphate
LMO	Lithium Manganese Oxide
NASA	National Aeronautics and Space Administration
NCM	Nickel Manganese Cobalt
Nom	Nominal
PE	Power Electronics
Prop	Propeller
PSEC	Power Specific Energy Consumption
PSFC	Power Specific Fuel Consumption
Req	Required
SOC	State of Charge
TO	Takeoff
VTOL	Vertical Takeoff and Landing
WTP	Well-to-Product/Pump
WTW	Well-to-Wheel

ABSTRACT

Yeung, Tsz Him, MSAE, Embry-Riddle Aeronautical University, May 2019. Optimal Battery Weight Fraction for Serial Hybrid Propulsion System in Aircraft Design.

This thesis focuses on electric propulsion technology associated with serial hybrid power plants most commonly associated with urban air mobility vehicles. While closed form analytical solutions for parallel hybrid aviation cases have been determined, optimized serial hybrid power plants have not seen the same degree of fidelity.

Presented here are the analytical relationships between several preliminary aircraft design objectives and the battery weight fraction. These design objectives include aircraft weight, range, operation cost, and carbon emissions. The relationships are based on a serial hybrid electric propulsion architecture from an energy standpoint, and can be applied to hybrid aircraft of different weights, aerodynamic designs, and propulsive efficiencies. Three hybrid electric propulsion design related variables are also defined in the process to help clarify novel specifications unique to hybrid propulsion systems. For all design objectives, the optimal battery weight fraction is found to be either zero or one in unconstrained cases. When a minimum range requirement is applied, non-integer weight fraction solutions can be found for minimizing cost and emissions.

1. Introduction

1.1. Motivation

With the advent of electric and hybrid electric propulsion systems in the automotive industry, electrification of aircraft propulsion systems has slowly gained popularity in recent years. Numerous aircraft manufacturers, such as The Boeing Company (Rayley, 2018) and the Airbus Group (Lyasoff, 2016), have begun research and development of hybrid electric or pure electric aircraft. Among these legacy manufacturers are also countless startup companies (Vertical Flight Society, 2019) that wish to explore the potential that a hybrid electric aircraft can bring.

One of the primary applications of hybrid electric aircraft is Urban Air Mobility (UAM), an on-demand passenger or cargo air transport system. Due to their architecture, hybrid propulsion systems enable a new category of aircraft, known as Vertical Take-off and Landing (VTOL), that fits between conventional general aviation (GA) aircraft and helicopters. As the name suggests, VTOL aircraft are capable of taking off and landing vertically, in contrast to aircraft that require significant space to accelerate and take-off. Yet, it differs from helicopters in that VTOL aircraft can be more efficient for long distance travel, and cheaper for mass scale use. According to a study conducted by Uber (Uber Technologies Inc, 2016), a worldwide transportation network company, an average San Francisco resident spent approximately 230 hours a year traveling between work and home, which is approximately half a million hours of productivity lost every day collectively for the city. They believe that VTOL aircraft can be the solution to such inner-city travel problems. Furthermore, in addition to the benefits over GA aircraft and helicopters mentioned above, hybrid electric enabled VTOL aircraft have a lower noise

signature, little to no operational carbon emissions for full electric cases, and can be much safer. These are critical criteria for flights within an urban environment.

In designing hybrid electric aircraft, one of the first challenges is properly sizing the battery. In the past, conventional aircraft obtained their energy from burning jet fuel. With the introduction of an electrical system as a method of propulsion for hybrid electric aircraft, batteries become a candidate for an alternate source of energy. Unlike jet fuel, however, the size and weight of battery has a direct impact on power delivery. For any power and capacity requirement, a study has found that there are governing equations that dictate the configuration and minimum size of a battery used for propulsive purpose (Zhao, 2018). These equations take into account variables including the battery state of charge and discharge current to ensure the battery configuration is capable of delivering the required amount of power. Additionally, miscellaneous components that make up the battery pack, such as the battery management or cooling system, must also be considered. For example, for the Diamond HK-36 electric aircraft at the Eagle Flight Research Center (EFRC) at Embry-Riddle Aeronautical University, it is estimated that the battery cells only account for 58% of the weight in a battery pack (Lilly, 2017). This means that a factor must be applied to the minimum battery weight to account for the weights of other components.

With the battery properly sized, the amount of fuel that should be carried onboard is the next challenge. At the time of this writing, lithium ion batteries only contain approximately one-sixtieth (1/60) of the energy compared to kerosene type jet fuel of the same mass, or one-eighteenth (1/18) of the energy for the same volume (Hepperle, 2012). If increasing battery weight means reducing the amount of fuel on board to maintain the

same energy weight fraction, aircraft range and endurance will decrease drastically. Using a modified form of Breguet's range equation, closed form analytical solutions have been developed to estimate the range for hybrid electric aircraft in recent years (Marwa et al, 2017). The solution takes into account the hybrid configuration, energy weight fraction, and different flight schedules to predict the range of an aircraft that is fully electric or jet fuel powered, and any hybrid configuration in between. Among these variables, the ratio between the weights of the battery and fuel has one of the most significant impact on the range outcome.

Although the studies mentioned above provide a clear guideline on how to size the battery and fuel system for expected power or range result. It is still unclear what the optimal battery weight fraction is. For instance, if one's goal is to minimize the emissions of an aircraft using hybrid propulsion technology, there is no well-defined solution for such type of design objectives at the current stage. Leveraging existing findings, it is the goal of this study to formulate a battery weight solution that can optimize aspects that hybrid electric propulsions excel at, such as operating cost and emissions, while allowing them to be operationally feasible regarding range and endurance.

1.2. Problem Statement

Electric motors in serial hybrid electric propulsion systems enable novel propulsion technologies, such as distributed propulsion and decoupling of motor RPM and torque. The addition of batteries as a second source of energy enables another level of redundancy and a quicker system dynamic response. Together, these designs enable flight missions in an urban environment due to the possibilities of a lower noise signature, VTOL capability, and increased safety. However, a significant drawback of hybrid

electric propulsion systems is current batteries' low specific energy and power compared to aviation fuel. This discrepancy prohibits new hybrid architecture designs to solely rely on the battery as a prominent source of energy due to the increase in weight. It is the major effort of this work to find the optimal battery weight fraction for a given range requirement that can enable serial hybrid propulsion as a feasible solution.

1.3. Objectives

1.3.1. General Objectives

The goal of this study is to provide a guideline on how to obtain the optimal battery weight fraction for a propeller driven serial hybrid aircraft in the preliminary design stage. This is completed via formulating relationships between battery weight fraction and multiple common design objectives. Then, if a feasible solution exists, identify the weight fraction for which the objective can be minimized or maximized. The study also aims to relate the specific objectives to a specified range requirement.

1.3.2. Specific Objectives

Define functional variables that aids in hybrid propulsion system design

With the added electrical and battery system, it is necessary to identify critical hybrid-related design parameters similar to 'wing loading' or 'empty weight fraction' in conventional aircraft design. Such variables should be applicable to any hybrid propulsion system design and help with comparison between different designs.

Formulate relationship between weight, range, cost, and emissions with battery weight fraction

Aircraft designs often have to satisfy specific mission requirements. Developing relationships between these common design objectives can provide a top-level guideline

on properly sizing the battery and fuel weight. Relationships should be developed with parameters that account for different aircraft designs, such that they are universally applicable.

Define the optimal battery weight fraction point or trend for each objective

Under the serial hybrid propulsion architecture, the aforementioned relationships are evaluated for different battery and fuel weights to obtain the ratio that optimizes the objective. The result should serve as a guideline on whether to increase or decrease the ratio for better performance outcome.

Identify possible battery sizing constrains due to operational requirements

In addition to design objectives, there are mission requirements that will directly impose constraints on the range of possible battery size. These constraints should be identified along with any equations that compute the boundaries.

Identify steps in optimizing multi-objectives design

If there are more than one design objectives that need to be considered, the order for applying the relationships and constraint equations to obtain the optimal battery weight fraction should be specified.

2. Literature Review

2.1. Hybrid Electric Propulsion Systems

Hybrid electric propulsion systems can be classified as a branch of alternative propulsion technologies. In the same category are other forms of technologies that do not follow the conventional propulsion design paradigm. Examples include alternative fuels or propulsion systems that utilizes solar energy (Storm et al, 2007). In general, alternative propulsion describes areas of ongoing research that can improve some aspects of flight. More examples of alternative propulsion for aviation can be found in Figure 2.1 (Gartenberg, 2017).
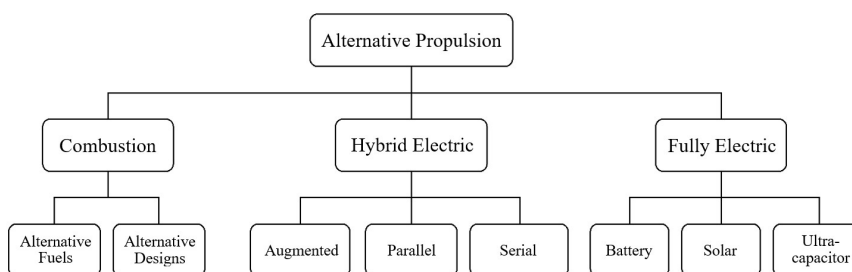
Figure 2.1. Alternative propulsion tree.

Any propulsion system that utilizes both a conventional combustion engine and an electric motor for the purpose of propulsion can be classified as a hybrid electric propulsion system. In most cases, batteries and jet fuel are used as the two primary sources of energy onboard. However, there are also specific design cases that favor one energy source over the other, and, therefore, only one is used.

Currently, there are two prevalent forms of hybrid propulsion systems, which are parallel hybrid and serial hybrid (Emadi at el, 2008). As their names suggest, parallel hybrid architecture has the gas engine working in parallel with the electric motor to deliver propulsive power, while serial hybrid's engine and electric motor are in series

with each other. Figure 2.2 below depicts an example of a parallel hybrid system.

Fuel — Engine — Generator — Rectifier — Inverter — Electric Motor — Gearbox — Battery
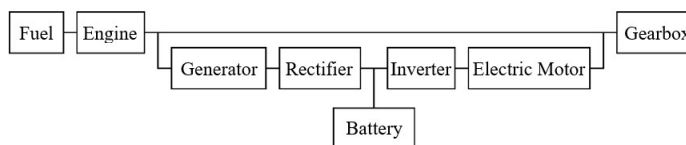
Figure 2.2. Example parallel hybrid propulsion system architecture.

For the parallel architecture, the gas engine and electric motor are connected through a gearbox, which in turn delivers power to the propeller. If properly sized, either the engine or the motor can power the aircraft by itself. This provides redundancy in case either system fails. Since both systems are directly connected to the propeller, compared to serial hybrid, parallel hybrid tends to have a better overall system efficiency. This means that it excels at travelling a further distance while reducing cost and emissions from consuming fuel or electricity (Eckert at el, 2015). However, due to the coupling nature of the system, the gas engine cannot always operate at its optimal design point while both systems are producing power. For that, serial hybrid architecture, as shown in Figure 2.3, offers a better solution.

Battery

Fuel — Engine — Generator — Rectifier — Inverter — Electric Motor
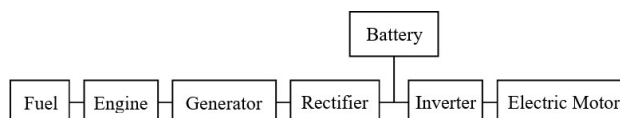
Figure 2.3. Example serial hybrid propulsion system architecture.

For the serial architecture, it is immediately obvious that the engine is no longer directly connected to the propeller. Rather, it provides electrical power via a generator to the electric motor for propulsion. This implies that the gas engine will suffer from stacking of inefficiencies from the generator, power electronics, and the electric motor when acting as the prime mover of the system. Therefore, serial hybrids are more suited for short missions, such as in urban environments, that will minimize loss. In addition,

the electric motor provides more flexibility in choosing the optimal propeller RPM and torque for quiet flight (Gartenberg, 2017).

Since the systems are coupled electrically, serial hybrid propulsion systems enable different aircraft designs, such as distributed propulsion. The architecture allows a gas engine operating at its optimal design point to provide power to smaller, lighter, and more efficient electric motors for propulsion (Kim, 2010). With proper propeller and aircraft design, serial hybrid provides the possibility of larger sized quadcopter-like aircraft that can carry heavy payloads.

2.2.   Energy Sources and Specific Energy

Two most commonly used aircraft fuels in the U.S. are AVGAS 100LL and Jet A. AVGAS 100LL is commonly used by general aviation aircraft; whereas Jet A is used by turbine-powered aircraft such as large commercial airliners. Whether it is for a small piston engine or a powerful turbofan engine, jet fuel will reliably provide a predictable and consistent amount of power throughout the mission. Their respective specific energy values are shown below in Table 2.1 (Air BP, 2000).

Table 2.1.

Aviation fuel weight specific energy

Fuel Type	Specific Energy [kWh/kg (HP-hr/lb)]
AVGAS 100LL	12.15 (7.39)
Jet A	11.95 (7.27)

A higher specific energy dictates that, for the same weight, it is possible to extract more energy from that resource or, conversely, the energy weight will be lighter for the same energy requirement.

For batteries, a Panasonic NCR18650B (Panasonic, 2012) and a Kokam Superior

Lithium Polymer Battery (Kokam, n.d.) are chosen for comparison due to their rising popularity in hybrid electric propulsion applications. From the respective companies' data sheets, the batteries' weight specific energies are shown in Table 2.2.

Table 2.2.

Aviation battery weight specific energy

Fuel Type	Specific Energy [kWh/kg (HP-hr/lb)]
Panasonic NCR18650B	0.243 (0.148)
Kokam SLPB080085270	0.260 (0.158)

As seen from the above tables, the weight specific energy of batteries are approximately two orders of magnitude lower than that of the aviation fuels'. Moreover, the power a battery can provide varies and depends on numerous parameters such as state of charge, cycle life, C-rate, and its chemical composition (Reddy, 2011). Therefore, not all the energy can be extracted from the battery.

From a weight standpoint, it is more desirable to use a jet fuel powered propulsion system versus a battery powered system until the specific energy of batteries attains a sustainable value. Assuming a constant yearly improvement between 3-7% for Li-ion batteries, Figure 2.4 shows the estimated time it will take for that to happen.
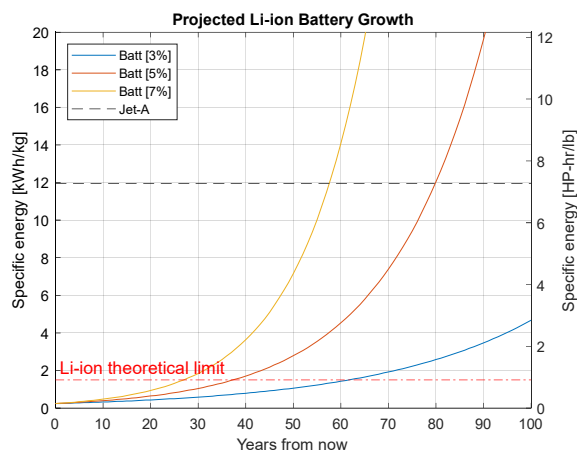
Figure 2.4. Projected Li-ion battery growth.

Barring any unexpected drastic battery development, the plot shows that it would take at least 50 years for Li-ion battery to have the same specific energy as Jet A fuel. More importantly, it is impossible chemically for Li-ion batteries to even reach that point as indicated by the theoretical limits on the plot (Reddy, 2011). For that reason, the size of the battery must be chosen properly to avoid carrying unnecessary weight.

If the control volume is expanded to the propulsion system, and assume a 'system specific energy' that is expressed as:

$$\rho_{sys} = \frac{E_{batt} + E_{gas}}{W_{batt} + W_{gas} + W_{system}} \tag{2.1}$$

then a plot of weight versus system specific energy can be generated, such as the one shown in Figure 2.5, to show the minimum system weight for a given power requirement. The weight of the system is computed based on previous study on the weights of currently available engines and electric motors conducted at the EFRC.
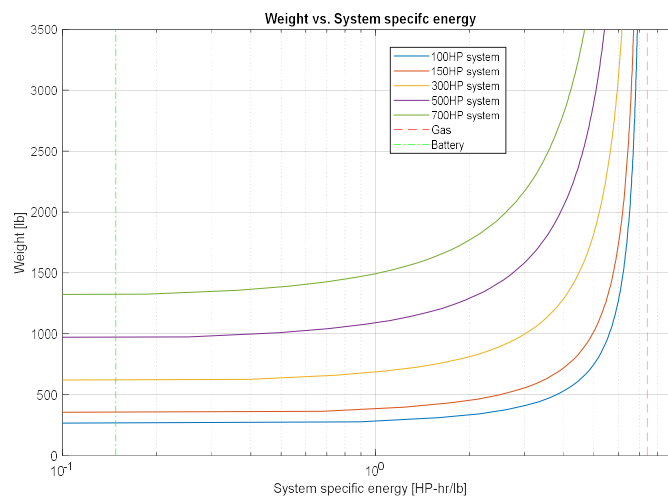
Figure 2.5. Weight vs. System specific energy (gas only).

Starting with no energy on board, the system specific energy will be zero. Then, as more and more gas is added, the specific energy of the system will approach that of

gasoline. Eventually, the weight of the system will increase exponentially since the system specific energy cannot be higher than that of gasoline. This indicates that if one wants to design a serial hybrid propulsion system capable of producing 500 HP for example, it is impossible to have a weight lower than about 1,000 lbs. As the energy requirement increases, the minimum weight must also increases.

2.3. Cost

According to the Annual Energy Outlook 2019 report published by the U.S. Energy Information Administration (2019), the projected price for electricity and jet fuel in 2019 are presented below in Table 2.3.

Table 2.3.

Cost of electricity and gasoline

	Cost [$/kWh]	Compare to Electricity
Electricity	0.11	-
Jet fuel	0.047	42.7%

Table 2.3 shows that consuming gasoline will provide a cheaper cost per unit of energy. The projected cost of jet fuel and electricity for the future 30 years can also be found and presented in Figure 2.6.
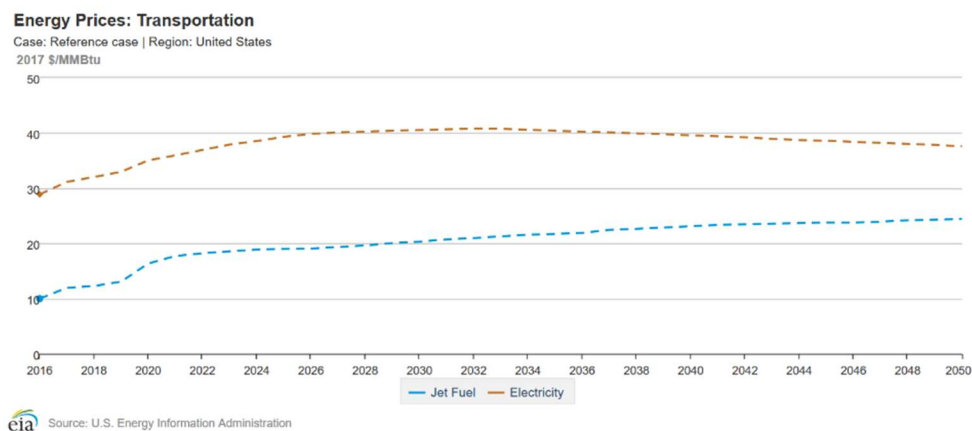
Figure 2.6. Projected cost of jet fuel and electricity (2016 – 2050).

Although the cost of electricity appears to be slowly converging to that of jet fuel, it can be expected that the cost per unit energy of fuel will still be lower than that of electricity in the foreseeable future.

2.4. Greenhouse Gas Emissions

For a hybrid aircraft, greenhouse gas (GHG) is generated due to consuming electricity and gasoline during the mission. For each resource, it is necessary to differentiate the actual source of GHG emissions. For example, prior to the consumption of jet fuel in an aircraft, "crude oil drilling, pumping, refining, and shipping contribute to the carbon footprint of gasoline" (Argonne National Laboratory [ANL], 2012). The GHG contribution due to this chain of action is commonly generalized as the Well-to-Product or Well-to-Pump (WTP) emissions. After the product arrives at the pump ready to be used, emissions due to actually burning the gasoline are then referred to as Pump-to-Wheels. This is often what the general public think of regarding GHG emissions from gasoline. Nonetheless, the addition of the two segments should be considered as the actual emissions due to consuming gasoline, and it is known as the Well-to-Wheels (WTW) emissions. A pictorial representation of this process is shown in Figure 2.7. For electricity, no GHG is emitted while it is being used. Therefore, the WTW emission is simply the WTP emission in all cases.
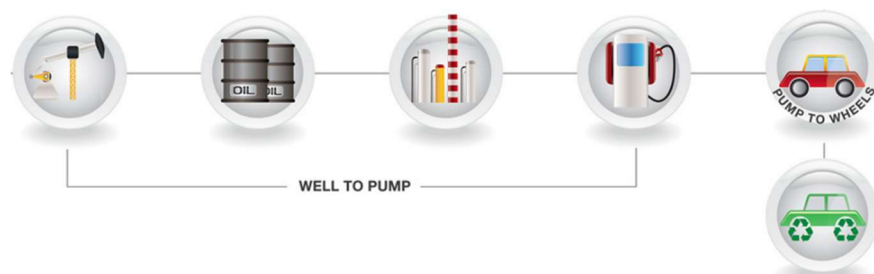
Figure 2.7. Depiction of gasoline's Well-to-Wheels emissions cycle (ANL, n.d.).

One of the most comprehensive studies on emissions output of various vehicle and energy source can be found within the Greenhouse gases, Regulated Emissions, and Energy use in Transportation (GREET) model developed by the Argonne National Laboratory (2018). It is a project sponsored by the U.S. Department of Energy, and provides extensive data on the life cycle emissions of numerous energy sources such as gasoline, natural gas, biofuel, electricity etc.

Using the results provided by the GREET model (ANL, 2018), Figure 2.8 shows jet fuel's Well-to-Pump and Pump-to-Wheel emissions contribution for three different oil sources and the national average.
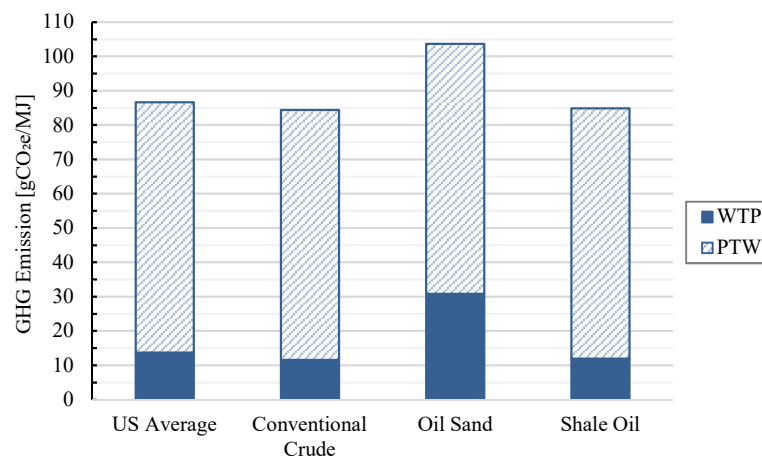
Figure 2.8. Greenhouse gas emissions (Jet Fuel) from different sources.

Similarly, for electricity, Figure 2.9 shows the equivalent carbon dioxide emissions due to multiple methods of generating the electricity. Recall that no GHG is emitted while using the electricity, therefore, PTW emission values are zero for all cases.
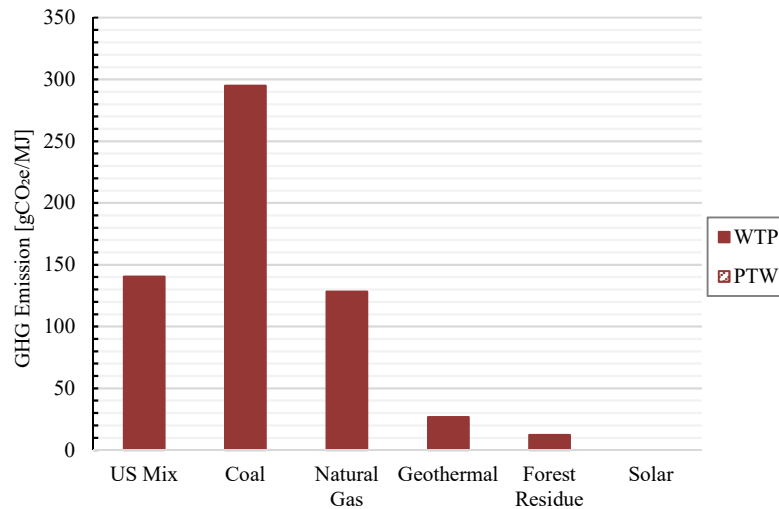
Figure 2.9. Greenhouse gas emissions (Electricity) from different sources.

Here, "US Mix" represents the weighted average of multiple pathways that the U.S. is generating electricity. Obviously, if one resides in an area where burning coal is the major method of generating electric, the emission consequences of operating an electric aircraft is much higher than operating at areas where electricity is generated using renewable methods. Table 2.4 shows the difference in WTW emission between the two sources and common fuel used by automotive (ANL, 2018).

Table 2.4.

Well-to-Wheels emission comparison

Resource	WTW Emission [gCO₂e/MJ]
Electricity	140
Jet fuel	87
Gasoline (Car)	93
Diesel (Car)	94

For reference in commonly used units, that is approximately 504 gCO_2e/kWh for consuming electricity and 11,370 gCO_2e/US gallon for consuming Jet A fuel. Additionally, be reminded that the values presented in Table 2.4 are comparing their

emission based on pure energy content. This is not equivalent to the shaft power each energy source can provide, which depends on the propulsion systems' efficiency.

In addition to GHG emitted during the mission, total emissions includes the carbon footprint of manufacturing the base components, namely the lifecycle emissions of making lithium ion batteries. A study conducted by the International Council of Clean Transportation investigates and compares the overall carbon dioxide emissions between conventional, hybrid electric, and fully electric cars found in Europe. One of the results from the report is presented in Figure 2.10.
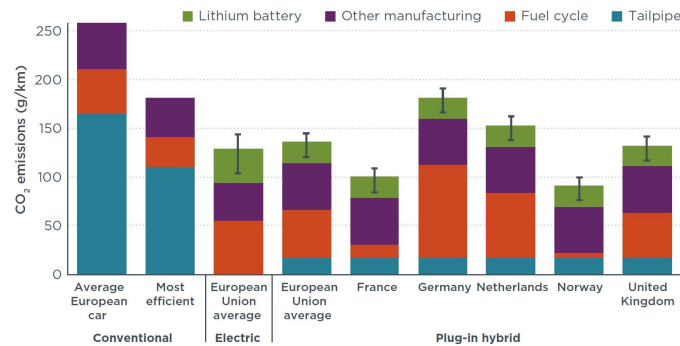
Figure 2.10. Comparison of life-cycle GHG emissions in European markets (Hall & Lutsey, 2018).

Here, the 'Lithium battery' portion refers to the carbon dioxide emitted during battery production. Therefore, observing the second through fourth column of the chart, it can be deduced that electric vehicles have the lowest total emissions, followed by hybrid, then conventional gas engines. Since the WTW emission values for gasoline and jet fuel are comparable as shown in Table 2.4, and lithium battery is mostly the same for propulsion applications, the result would be similar for hybrid electric aircraft.

Another study conducted at Tsinghua University in China shows the actual equivalent carbon emission values due to battery manufacturing from different sources for multiple battery composition. A summary chart is shown in Figure 2.11.
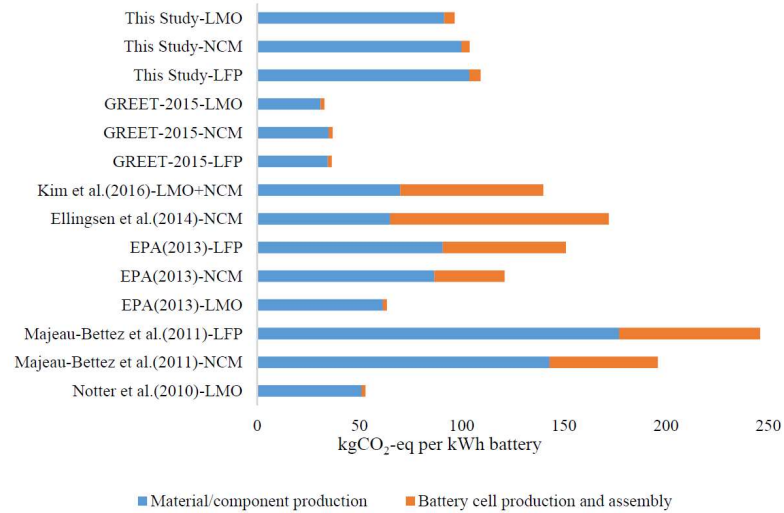
Figure 2.11. Equivalent CO_2 emissions due to battery manufacturing (Hao et al., 2017).

In Figure 2.11, 'LMO', 'NCM', and 'LFP' refers to different types of lithium ion batteries. As indicated in the figure, there is a significant discrepancy between different studies even for the same battery type. For LFP battery, the emission figure reported by Majeau-Bettez et al is more than five times higher than that reported by the GREET model. This shows that different methods of gathering data and developing the approximation model can have a substantial impact on estimating carbon emissions due to battery production.

3. Methodology

3.1. Serial Hybrid Modes of Operation

Three power delivery paths are considered in this study and shown in Figure 3.1. Each describes how the chemical energy from the jet fuel or batteries are converted to mechanical energy used to power the propeller. The first two shown are direct paths from the fuel and batteries to the propeller. Whereas the last one represents a jointed operation, where the gas is used to charge the battery, which then powers the propeller.

(a) Gas to Propeller:
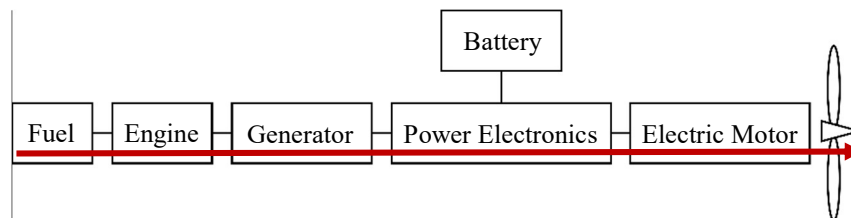
(b) Battery to Propeller:
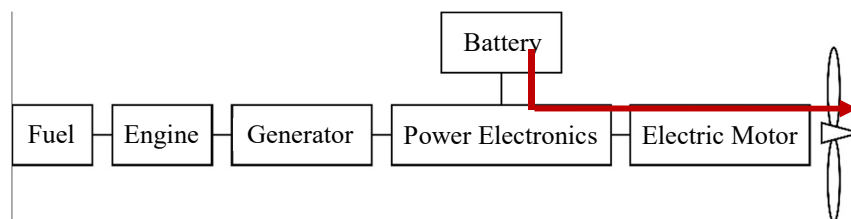
(c) Air-charging:
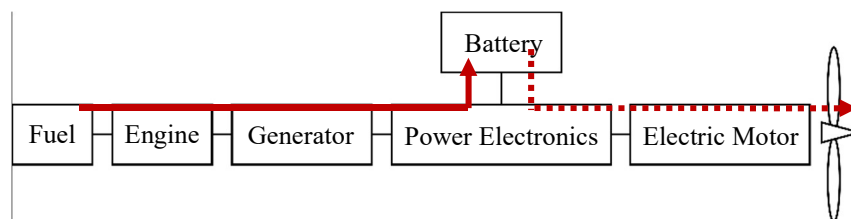
Figure 3.1. Serial hybrid propulsion system power delivery paths.

Each of these modes is mathematically modeled as a product of the involved components' efficiencies, shown below in Equation (3.1) to (3.3) in the order they are presented.

$$\eta_{gas \to prop} = \eta_{eng}\eta_{gen}\eta_{PE}\eta_{EM}\eta_{prop} \tag{3.1}$$

$$\eta_{batt \to prop} = \eta_{batt}\eta_{PE}\eta_{EM}\eta_{prop} \tag{3.2}$$

$$\eta_{charge} = \eta_{eng}\eta_{gen} \tag{3.3}$$

For the purpose of generating plots in the following sections, the efficiency values presented in Table 3.1 are used. They are approximated generic values and can be replaced with any desired value if a specific propulsion component is chosen.

Table 3.1.

Assumed efficiency values

Symbol	Component	Value
η_{eng}	Gas engine	0.3
η_{gen}	Generator	0.9
η_{PE}	Power electronics	0.95
η_{batt}	Battery	0.9
η_{EM}	Electric Motor	0.9
η_{prop}	Propeller	0.8

Note that the efficiency of the battery refers to the amount of stored energy that can be extracted from the cell. This value is dependent on the current being drawn from the battery among other variables.

The main focus of this study will be placed on disjointed operation, as shown by case (a) and (b) in Figure 3.1, where the fuel and battery are used independently of each other. It is assumed that either the gas engine or the battery powered electric motor will provide all the power at any point during the flight, meaning the two systems are never used

simultaneously. The reason for this, is to understand the direct impact of variation in battery weight fraction. At the end of the chapter, the impact of air-charging will be explored.

3.2. Hybrid Variables Definition

Energy weight in a conventional fully gasoline power aircraft is equivalent to the fuel weight, where all the energy onboard comes from the fuel source. For a hybrid electric aircraft, however, the energy weight is the combined weight of fuel and battery. Therefore, a new variable – Energy Weigh Fraction (β) is defined as the ratio between the energy weight and the aircraft weight to quantify the total amount of energy onboard as follows:

$$\beta = \frac{W_{energy}}{W} = \frac{W_{gas} + W_{battery}}{W} \tag{3.4}$$

Next, Percent Hybrid (x) will be used to quantify the battery weight in relationship with the fuel weight and the energy weight. It is defined as the ratio between the battery weight and the energy weight:

$$x = \frac{W_{battery}}{W_{energy}} \tag{3.5}$$

One of the benefits of using percent hybrid over the battery weight is its unitless property. When comparing between two hybrid aircraft designs that have different weights, percent hybrid can help to communicate the relative energy content onboard.

Using the two defined variables, the weight of battery and gasoline can be expressed in terms of the aircraft weight as:

$$W_{battery} = x \cdot W_{energy} = x\beta W \tag{3.6}$$

$$W_{gas} = (1 - x)W_{energy} = (1 - x)\beta W \tag{3.7}$$

Lastly, charging fuel weight fraction (α) is defined as the weight fraction of fuel

dedicated to charging the battery, as opposed to propulsion:

$$\alpha = \frac{W_{gas,charge}}{W_{gas}} \tag{3.8}$$

The charging fuel weight fraction allows the remaining study to analyze the relationships

between any objective and percent hybrid from an energy standpoint. This means that the

results of this study will remain valid regardless of the mission's power profile, as long as

the overall energy usage is correctly depicted using these variables.

As mentioned before, since this study will be focused on disjointed cases, it can be

assumed that $\alpha = 0$ unless otherwise stated. However, for completeness, all the

derivations will still include the charging fuel weight fraction.

The diagram shown below in Figure 3.2 illustrates the relationship between the three

variables.
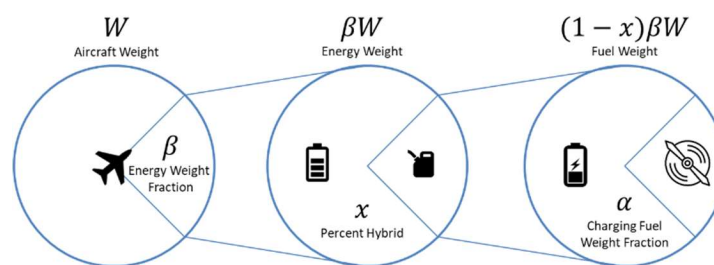
Figure 3.2. Hybrid variables definition.

As all three newly defined variables are weight fractions, their permissible ranges are

from 0 to 1. For clarity, Table 3.2 presents the exact meaning for these variables at their

extrema.

Table 3.2.

Hybrid variables definition at extrema

Variable	Meaning at 0	Meaning at 1
Energy weight fraction (β)	No weight on the aircraft is dedicated towards battery and/or gas.	The entire aircraft weight consists only of battery and/or gas.
Percent hybrid (x)	Aircraft is fully powered by gasoline.	Aircraft is fully powered by batteries.
Charging fuel weight fraction (α)	All the fuel on board is used for propulsion.	All the fuel on board is used to charge the battery.

3.3.   Weight Optimization

In aircraft design, it is often desirable to minimize the overall weight of the aircraft for better performance, and one significant weight contribution is the weight of fuel and batteries. The amount of fuel and batteries needing to be carried is determined by the energy required to complete the mission. Therefore, the sum of the energy provided by the two sources must equal a given energy requirement:

$$E_{req} = E_{batt} + E_{gas} \tag{3.9}$$

The amount of energy that can be extracted from the energy sources is the product of their respective weights and specific energy. Accounting also for the loss in converting the energy sources to mechanical energy, the corresponding efficiency term are added:

$$E_{req} = W_{batt}\rho_{batt}\eta_{batt \to prop} + W_{gas}\rho_{gas}\eta_{gas \to prop} \tag{3.10}$$

The energy from the gasoline can be used for charging the battery or to power the propeller directly, and the loss is different for the two cases. Subsequently, the efficiency term associated with gasoline's energy is adjusted depending on the ratio of gasoline used for charging. On the other side of the equation, the energy requirement for the mission can be computed as the average power required times the duration of the mission. Therefore, Equation (3.10) can be rewritten as:

$$P_{avg} \cdot t = W_b \rho_b \eta_{b \to p} + W_g \rho_g \left[(1 - \alpha) \eta_{g \to p} + \alpha \eta_{charging} \eta_{batt \to prop} \right] \qquad (3.11)$$

Note that if all the fuel is used directly to power the propeller, meaning no air-charging

occurs during the entire flight, α would be equal to zero in Equation (3.11) reverting to

the original form in Equation (3.10).

Finally, the fuel and battery weights can be related to the aircraft weight in terms of

percent hybrid and energy weight fraction as shown in Equation (3.6) and Equation (3.7),

resulting in the follow expression relating the aircraft weight and percent hybrid:

$$P_{avg} \cdot t = x \beta W \rho_b \eta_{b \to p} + (1 - x) \beta W \rho_g \left[(1 - \alpha) \eta_{g \to p} + \alpha \eta_{ch} \eta_{b \to p} \right] \qquad (3.12)$$

Since Equation (3.12) is a linear equation relating percent hybrid and weight of the

aircraft, it can be solved for either variable explicitly. If a target weight limit exists, the

percent hybrid required would be:

$$x = \frac{P_{avg} \cdot t - \beta W \rho_g \left[(1 - \alpha) \eta_{g \to p} + \alpha \eta_{ch} \eta_{b \to p} \right]}{\beta W \left[\rho_b \eta_{b \to p} - \rho_g \left((1 - \alpha) \eta_{g \to p} + \alpha \eta_{ch} \eta_{b \to p} \right) \right]} \qquad (3.13)$$

or if the percent hybrid is known due to other design objectives, the corresponding weight

would be:

$$W = \frac{P_{avg} \cdot t}{x \beta \rho_b \eta_{b \to p} + (1 - x) \beta \rho_g \left[(1 - \alpha) \eta_{g \to p} + \alpha \eta_{ch} \eta_{b \to p} \right]} \qquad (3.14)$$

Using the current specific energy of Li-ion battery and jet fuel shown in Table 2.1 and

Table 2.2, Equation (3.14) is plotted in Figure 3.3 for a disjointed case at a constant

energy weight fraction to show how varying percent hybrid can affect the weight.
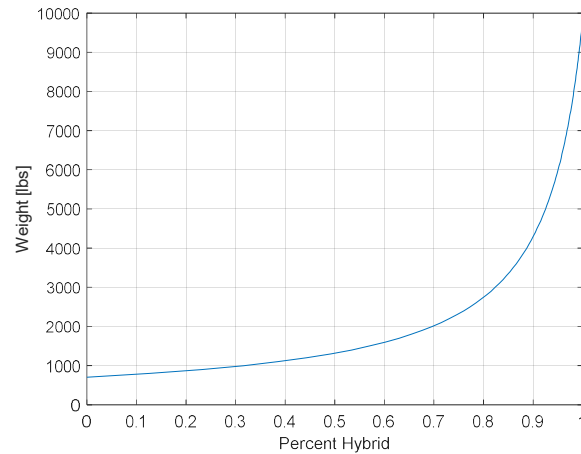
Figure 3.3. Minimum weight required vs. Percent Hybrid.

$$(\alpha = 0, \beta = 0.2, P_{avg} = 100HP, t = 2\ hrs)$$

Figure 3.3 shows that for a constant energy requirement, the minimum required weight of the aircraft will increase exponentially as percent hybrid approaches one. This is the minimum weight because any weight below that specified in Equation (3.14) will not have enough fuel and batteries to satisfy the power or endurance requirements. Therefore, to minimize weight for a constant energy requirement, it is desirable to minimize percent hybrid in most scenarios.

One exception to that is a high frequency charge-discharge cycle jointed serial hybrid operation. Assuming a mission power profile that has a continuous square wave power requirement, the peak power over an average power is provided by the battery and any power below average is used to charge the battery as shown by Figure 3.4:
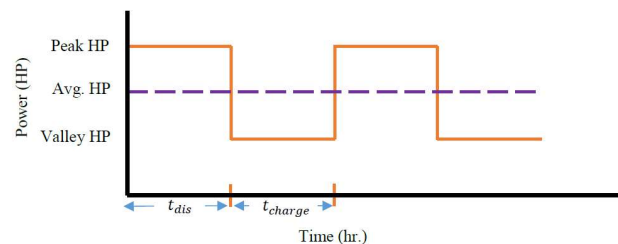
Figure 3.4. Example Peaks-and-Valley power profile (Rosales & Anderson, 2019).

Using empirical formulas to estimate the system component weights, a study compared the total weight difference between a fully gas-powered system that can satisfy the above power profile versus a gas and battery system. Under the assumption that the gas engine in the gas and battery jointed system will have approximately 2% better performance than that in a gasoline-only system, the study suggests that if the charge and discharge time are both below 10 minutes, a non-zero percent hybrid system can be lighter than a zero percent hybrid system in this case regardless of the power difference between the peaks and valleys (Rosales & Anderson, 2018). The actual percent hybrid value can be computed using the definition of percent hybrid shown in Equation (3.5), since the paper provided the equation for computing the battery and fuel weight.

However, the results from the study accounts for the weight of the entire propulsion system, as opposed to only the energy weight as shown in Figure 3.3. Therefore, further research might be needed to verify if it will still show the same trend if only the energy weight is considered.

3.4.   Range Optimization

The range of a serial hybrid electric aircraft can be expressed as the sum of the range provided by burning the gasoline and using the electricity in the battery:

$$R_{hybrid} = R_{gas} + R_{battery} \tag{3.15}$$

The range for gas will be derived using a modified form of the Breguet Range Equation, whereas the range for battery will be derived using its specific energy.

3.4.1. Gas Range

The range due to burning gasoline can be obtained by using the Breguet Range Equation. Starting with the definition of power specific fuel consumption (PSFC):

$$PSFC = \frac{dW_{fuel}/dt}{P} \qquad (3.16)$$

Assuming an equilibrium cruise condition, where lift generated by the aircraft is the same as the total weight, and power is the product of drag and velocity. Substituting and rearranging Equation (3.16) gives:

$$dt = \frac{1}{PSFC} \frac{dW_f}{D \cdot V} \frac{L}{W} \qquad (3.17)$$

To obtain range from Equation (3.17), multiply both sides by velocity and integrate. Note that the change in fuel weight is the same as the change in aircraft weight:

$$R_{gas} = V \cdot \int dt = \frac{1}{PSFC} \frac{L}{D} \int \frac{1}{W} dW \qquad (3.18)$$

For simplicity, it was assumed that the lift-to-drag ratio, which relates to aircraft's angle of attack, is constant regardless of weight. This means that the aircraft is climbing as the aircraft weight decreases over time.

To obtain the range given by the amount of fuel burned, integrate from final weight (W_2) to initial weight (W_1):

$$R_{gas} = \frac{1}{PSFC} \frac{L}{D} \int_{W_2}^{W_1} \frac{1}{W} dW = \frac{1}{PSFC} \frac{L}{D} \ln\left(\frac{W_1}{W_2}\right) \qquad (3.19)$$

Since the final weight is simply the initial weight of the aircraft subtracting the fuel burned for propulsion, it can be expressed as such:

$$W_2 = W_1 - W_{gas,propulsion}$$

$$= W_1 - (1 - \alpha)(1 - x)\beta W_1 \qquad (3.20)$$

$$= W_1[1 - (1 - \alpha)(1 - x)\beta]$$

Finally, substituting Equation (3.20) into Equation (3.19) gives the gas range as a function of PSFC and several nondimensionalized variables:

$$R_{gas} = \frac{1}{PSFC} \frac{L}{D} \ln\left(\frac{1}{1 - (1 - \alpha)(1 - x)\beta}\right) \tag{3.21}$$

To simplify further, realize that PSFC is a measure of how efficiently the gas engine can convert chemical energy from the gasoline to mechanical energy. Therefore, it is possible to express it as a Power Specific Energy Consumption (PSEC) as:

$$PSEC = PSFC \cdot \rho_{gas} = \frac{1}{\eta_{gas \to prop}} \tag{3.22}$$

In order to obtain the proper unit for range in the end, the specific energy has a unit of energy per weight (force) as shown in the two unit systems:

$$English\ unit: \frac{HP - hr}{lb_f}$$

$$SI\ unit: \frac{kWh}{N} \quad or \quad \frac{kWh/kg}{9.81\ ms^{-2}} \tag{3.23}$$

This unit definition applies to all specific energy variables from this point on. Substituting Equation (3.22) into Equation (3.21) and rearranging gives:

$$R_{gas} = \eta_{gas \to prop}\ \rho_{gas} \frac{L}{D} \ln\left(\frac{1}{1 - (1 - \alpha)(1 - x)\beta}\right) \tag{3.24}$$

which shows an explicit relationship between percent hybrid and the range provided by gasoline for a given efficiency and aircraft design. The resulting unit for range is feet in English units and meter in SI units.

3.4.2. Battery Range

Energy in the battery can come from two sources: when it is initially charged prior to the flight (ground-charge) or part of the gas is used to charge the battery during the flight (air-charge). The energy due to ground-charge can be calculated using the battery specific energy as shown:

$$E_{ground} = \rho_{batt} W_{batt} = \rho_{batt} x \beta W \qquad (3.25)$$

Similarly, the energy due to air-charge can be expressed as the product of fuel specific

energy and the fuel mass onboard for charging. Accounting for the loss during charging,

it can be expressed as:

$$E_{air} = \eta_{charge} \rho_{gas} W_{gas,charge} = \eta_{charge} \rho_{gas} \alpha(1-x)\beta W \qquad (3.26)$$

The total energy from the battery is, therefore, the sum of Equation (3.25) and Equation

(3.26), which simplifies to:

$$E_{batt} = \beta W \left[\rho_{batt} x + \eta_{charge} \rho_{gas} \alpha(1-x) \right] \qquad (3.27)$$

With the energy known, it is then possible to calculate the time it takes to fully

discharge the battery for a given power:

$$t_{discharge} = \frac{E_{batt}}{P} \qquad (3.28)$$

Assuming an equilibrium flight condition, Equation (3.28) can be rewritten as:

$$t_{discharge} = \frac{E_{batt}}{D \cdot V} \frac{L}{W} \qquad (3.29)$$

Lastly, multiply time to discharge with aircraft velocity to obtain the range due to

battery, and substituting Equation (3.27) in Equation (3.29) gives:

$$R_{batt} = \eta_{batt \to prop} \beta \frac{L}{D} \left[\rho_{batt} x + \eta_{charge} \rho_{gas} \alpha(1-x) \right] \qquad (3.30)$$

Again, an efficiency factor is added to account for the inefficiency for converting

electrical energy to mechanical energy.

3.4.3. Total Range Optimization and Linearization

With the range equations derived for burning gasoline and discharging the battery as

shown in Equation (3.24) and (3.30) respectively, the total range is simply the sum of the

two:

$$R = \frac{L}{D}\left\{\eta_{gas\to prop}\rho_{gas}\ln\left(\frac{1}{1-(1-\alpha)(1-x)\beta}\right)\right.$$

$$\left. + \eta_{batt\to prop}\beta\left[\rho_{batt}x + \eta_{charge}\rho_{gas}\alpha(1-x)\right]\right\} \tag{3.31}$$

One important thing here is how the total range is derived. The basis for Equation

(3.31) is computing how the chemical energy from both resources is converted to

mechanical energy. It does not take into account the aspect of converting the energy, such

as limitation on power delivery due to battery design. The equation assumes that all the

energy from the gasoline and battery can and will be used for propulsion or charging.

Therefore, Equation (3.31) should only be used to compute the theoretical maximum

range that can be extracted from the gasoline and battery.

For a constant energy weight fraction, Equation (3.31) is plotted at varying percent

hybrid in Figure 3.5.
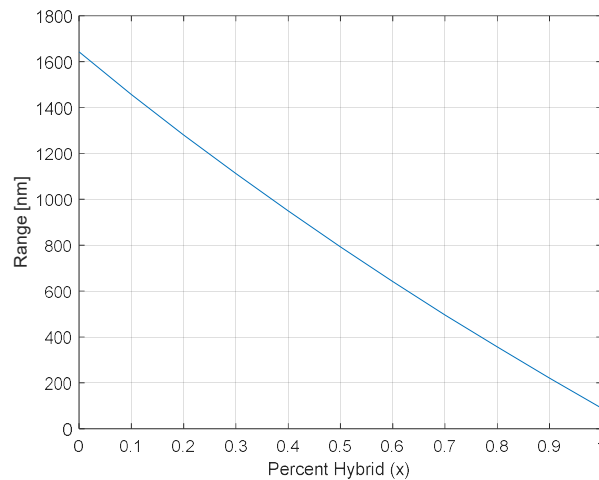

Figure 3.5. Range vs. Percent Hybrid.

$$(\alpha = 0, \beta = 0.3)$$

As shown from the plot, the range has drastically decreased by a factor of about 16

times when going from 0% to 100% hybrid for the example aircraft. This is to be

expected because going towards 100% hybrid is essentially replacing high specific energy jet fuel with low specific energy batteries. Since the weight of the aircraft is kept constant in this case, the overall energy onboard and, therefore, the range is reduced.

Although Equation (3.31) provides a direct relationship between range and percent hybrid, due the equation's nonlinearity, it is difficult to explicitly solve for the percent hybrid for a given range requirement. For that, a linearization process is done to provide an approximated close form solution.

First, recall that the natural logarithmic function can be approximated using the Taylor Series for all $|z| \leq 1$ and $z \neq 0$ as follows:

$$\ln(z) = (z - 1) - \frac{(z - 1)^2}{2} + \frac{(z - 1)^3}{3} \pm \cdots \tag{3.32}$$

Therefore, for a first-degree approximation, the logarithmic part in Equation (3.31) can be approximated as:

$$\ln\left(\frac{1}{1 - (1 - \alpha)(1 - x)\beta}\right) = -\ln(1 - (1 - \alpha)(1 - x)\beta) \approx (1 - \alpha)(1 - x)\beta \tag{3.33}$$

Substituting Equation (3.33) into Equation (3.31) gives:

$$R = \frac{L}{D}\{\eta_{g \to p}\rho_g(1 - \alpha)(1 - x)\beta + \eta_{b \to p}\beta[\rho_b x + \eta_{ch}\rho_g\alpha(1 - x)]\} \tag{3.34}$$

which is now a linear equation. Then, expanding Equation (3.34) and solving for the percent hybrid yields:

$$x = \frac{R - \frac{L}{D}\beta[\eta_{b \to p}\eta_{ch}\rho_g\alpha + (1 - \alpha)\eta_{g \to p}\rho_g]}{\frac{L}{D}\beta[\eta_{b \to p}(\rho_b - \eta_{ch}\rho_g\alpha) - (1 - \alpha)\eta_{g \to p}\rho_g]} \tag{3.35}$$

Though not as elegant, Equation (3.35) presents an explicit solution for maximum percent hybrid as a function of range desired, which is more useful in a design scenario. All impossible range requirements for the specified aircraft configuration will result in a

percent hybrid solution outside of 0 and 1 and should be discarded.

Using Equation (3.35), the maximum percent hybrid is plotted against range for three

different energy weight fractions in Figure 3.6.
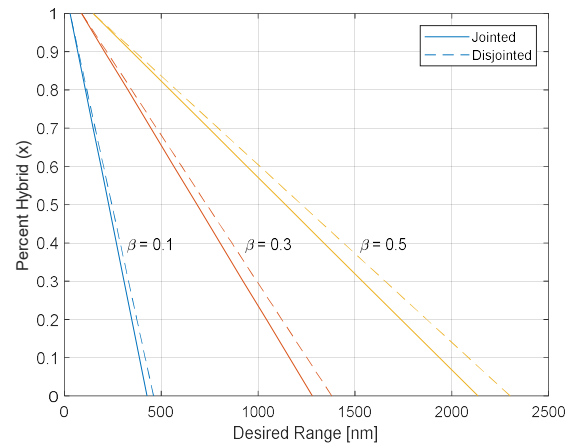
Figure 3.6. Percent hybrid vs. desired range.

($W = 5,000\ lbs., \alpha = 0.5$ for jointed)

Figure 3.6 will become significant in the following study because it gives the user a

way to obtain the upper bound for percent hybrid at any given range. Therefore, for any

objectives that are optimized when percent hybrid is maximized, it will be the optimal

percent hybrid. Lastly, a comparison between the range solutions found using the original

and linearized equation is shown in Figure 3.7.
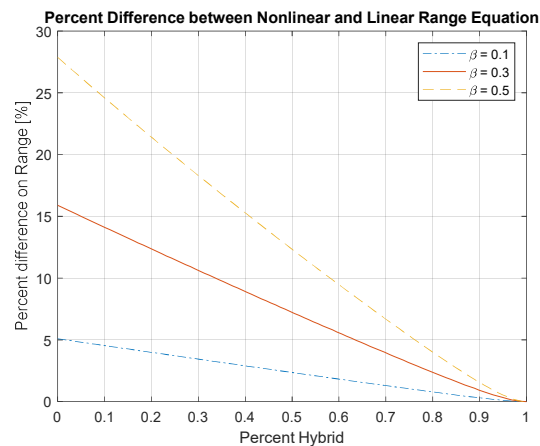
Figure 3.7. Percent Difference between Nonlinear and Linear Range Equation.

Evaluating the nonlinear and linear equations at different energy weight fractions and percent hybrid reveals that the first order linearized equation is best suited for cases with small energy weight fraction and high percent hybrid. This is due to the original Taylor Series approximation being linearized about $x = 1$ or $\beta = 0$. Therefore, deviation from these values will increase the percent difference.

A second order approximation can be used to reduce the error. However, Equation (3.35) may become too complicated to be used effectively. Another attempt to reduce the percent error is to linearize the logarithmic function around $x = 0.5$ and $\beta = 0.3$, which results in the percent difference plot shown in Figure 3.8.
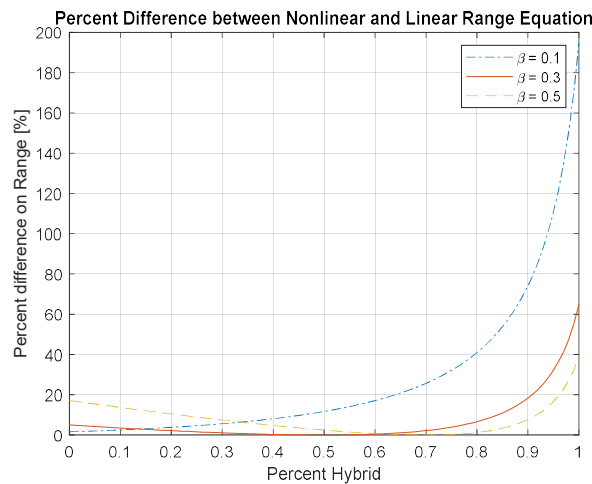
Figure 3.8. Percent Difference between Nonlinear and Linear Range Equation (Linearized around $x = 0.5$ and $\beta = 0.3$).

As seen, although the error has reduced at low percent hybrid for all energy weight fractions shown, the opposite end now shows more than a 40% percent difference between the linearized and the original equation. In addition to a simpler linearized form, the previous linearized point shows a better average percent difference. Therefore, it is concluded that the original linearization shown in Equation (3.33) is the best linearization approach.

3.5. Direct Operating Cost Optimization

As the name suggests, the direct operating cost (DOC) is solely the cost required to operate an aircraft for a specific flight. This term does not include other cost of aircraft subsistence such as maintenance cost or acquisition cost. For a gas driven system, the operating cost is simply the cost of purchasing and using the fuel. For an electric propulsion system, the DOC is the electricity used for charging the battery packs. Therefore, the DOC for a hybrid electric system can be expressed as:

$$Cost = x\beta W \rho_{batt} C_{batt} + (1-x)\beta W \rho_{gas} C_{gas} \tag{3.36}$$

where C_{batt} and C_{gas} are the cost of electricity and gas per unit of energy respectively.

Using the cost of electricity and jet fuel at the time of the writing presented in Table 2.3. The above equation is plotted at different percent hybrid in Figure 3.9.

Figure 3.9. Cost vs. Percent Hybrid.

$$(W = 5{,}000\ lbs., \beta = 0.3)$$

For a constant given weight, the cost of using a full gas system is more expensive than a fully electric system, despite electricity costs being more than double per unit energy than jet fuel. This is the case because jet fuel's high specific energy overcomes the

difference in price. For reference, one pound of gas increases the price by $0.26, whereas one pound of battery requires only $0.012 to charge. Therefore, to minimize direct cost of operation, it is desirable to maximize percent hybrid.
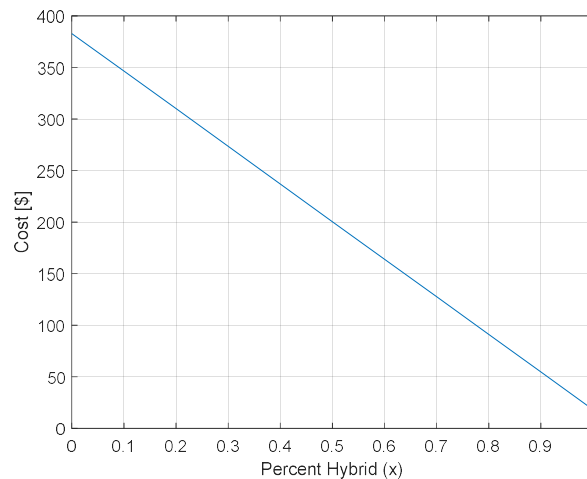
It is also possible to directly relate the cost equation to the range equation. To do so, simply substitute the resulting equation from linearizing the range equation shown in Equation (3.35) into the cost equation. For simplicity in the final equation, the percent hybrid is first factored out from the battery and gas term in Equation (3.36) as shown:

$$Cost = \beta W \left[x \left(\rho_{batt} C_{batt} - \rho_{gas} C_{gas} \right) + \rho_{gas} C_{gas} \right] \tag{3.37}$$

Then, substituting the expression for percent hybrid from Equation (3.35) yields

$$Cost = \beta W \left\{ \frac{R - \frac{L}{D} \beta [\eta_{b \to p} \eta_{ch} \rho_g \alpha + (1 - \alpha) \eta_{g \to p} \rho_g]}{\frac{L}{D} \beta [\eta_{b \to p} (\rho_b - \eta_{ch} \rho_g \alpha) - (1 - \alpha) \eta_{g \to p} \rho_g]} \cdot \left(\rho_b C_b - \rho_g C_g \right) + \rho_g C_g \right\} \tag{3.38}$$

Since Equation (3.36) accounts for the cost of electricity to charge the battery on the ground, Equation (3.38) will be the cost for a plug-in hybrid at the given range. For non-plug-in serial hybrid system, meaning that the battery is not charged at the beginning of the flight, a similar cost equation can be obtained by simply neglecting the battery term in Equation (3.36) then substituting in the percent hybrid expression:

$$Cost = \left(1 - \frac{R - \frac{L}{D} \beta [\eta_{b \to p} \eta_{ch} \rho_g \alpha + (1 - \alpha) \eta_{g \to p} \rho_g]}{\frac{L}{D} \beta [\eta_{b \to p} (\rho_b - \eta_{ch} \rho_g \alpha) - (1 - \alpha) \eta_{g \to p} \rho_g]} \right) \beta W \rho_g C_g \tag{3.39}$$

The costs given by Equation (3.38) and Equation (3.39) are the optimal cost for the given range. This is because the percent hybrid given by Equation (3.35) is the maximum allowed percent hybrid that will satisfy the range requirement. This coincides with the optimized trend for cost, which is to maximize the percent hybrid. The optimal cost is plotted for the example aircraft at different desired range in Figure 3.10.
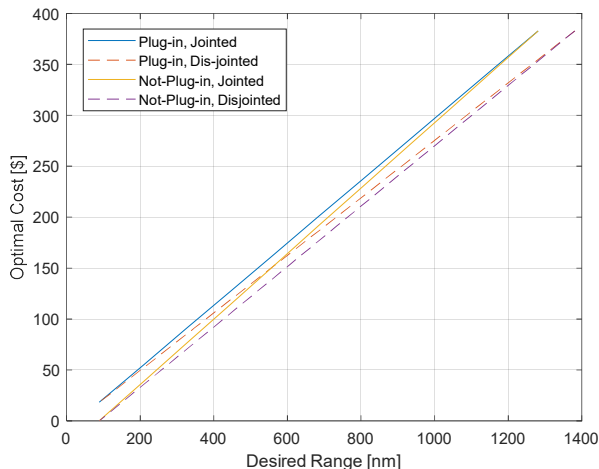
Figure 3.10. Optimal Cost vs. Desired Range

($W = 5,000 \, lbs., \beta = 0.3, \alpha = 0.5$ for jointed).

The figure illustrates that the higher the desired range, the higher the direct operating cost will be. This reflects the combined trend of the range and cost equations, where the lowest cost occurs when percent hybrid is maximized, corresponding to the shortest range in Figure 3.10.

To understand and compare the average cost of the mission, another metric of interest is the cost per distance traveled. This can be computed by dividing the cost by the range input, the result from the example aircraft is shown in Figure 3.11.
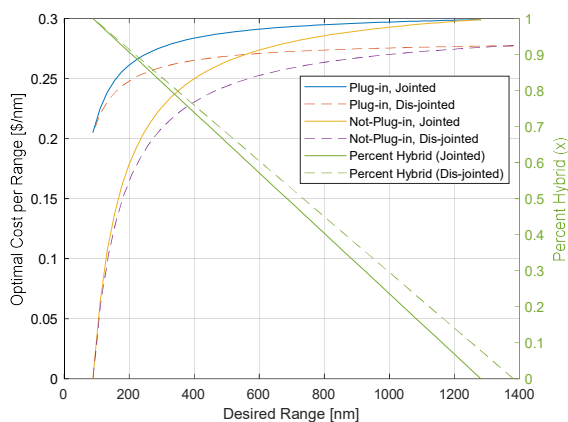
Figure 3.11. Optimal Cost per Range vs. Desired Range.

($W = 5,000 \, lbs., \beta = 0.3, \alpha = 0.5$ for jointed)

The percent hybrid is also shown in Figure 3.11 for the corresponding range. In the figure, it indicates it is more economical to travel per nautical mile when operating a fully electric aircraft, where there is a significant drop off in price in exchange for the low range. On the other hand, it can be seen that the cost per nautical mile stays relatively constant at higher desired range, especially for the plug-in cases.

3.6. Emission Optimization

3.6.1. Mission Emission

A similar approach may be used to compute the carbon emissions released during the mission or flight. Assuming all the energy onboard is consumed, the emission is the sum of the emissions due to charging the battery, and consuming the gasoline:

$$Emission = x\beta W \rho_{batt} K_{batt} + (1 - x)\beta W_{gas}\rho_{gas} K_{gas} \qquad (3.40)$$

where K_{batt} and K_{gas} are the carbon emissions due to charging battery and consuming gas per unit of energy. Since both the operating cost and emissions are directly proportional to the amount of energy onboard the aircraft, Equation (3.40) shows a similar structure to the cost equation shown in Equation (3.36). This means that a similar result between the two can be expected.

Using the electricity and jet fuel emission values shown in Table 2.4, Figure 3.12 depicts the emissions computed using Equation (3.40) at different percent hybrid.
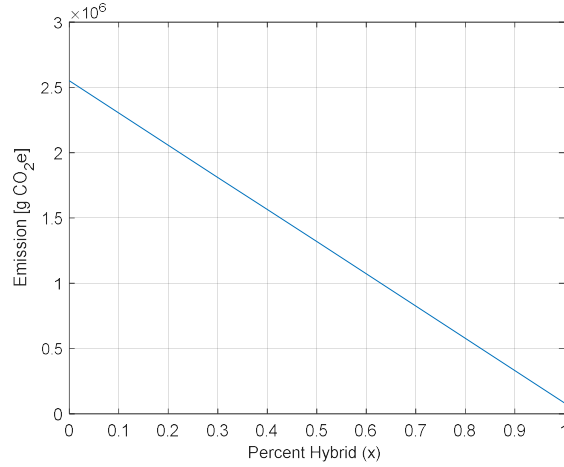
Figure 3.12. Emission vs. Percent hybrid.

$$(W = 5{,}000 \ lbs., \beta = 0.3)$$

Despite consuming electricity on average producing more carbon emissions, due to battery's low specific energy compared to that of the gasoline, using a full electric system resulted in a lower overall emissions. At the same time, however, since the weight remains constant, the range will decrease. To understand the relationship between emission and range, a similar approach, as in the cost section, can be used. First, isolate percent hybrid in Equation (3.40):

$$Emission = \beta W \left[x \left(\rho_{batt} K_{batt} - \rho_{gas} K_{gas} \right) + \rho_{gas} K_{gas} \right] \tag{3.41}$$

Then, substitute in Equation (3.35) for percent hybrid as a function of range:

$$Emission = \beta W \left\{ \frac{R \ - \frac{L}{D}\beta\left[\eta_{b\to p}\eta_{ch}\rho_g\alpha + (1-\alpha)\eta_{g\to p}\rho_g\right]}{\frac{L}{D}\beta\left[\eta_{b\to p}\left(\rho_b - \eta_{ch}\rho_g\alpha\right) - (1-\alpha)\eta_{g\to p}\rho_g\right]} \cdot \left(\rho_b K_b - \rho_g K_g\right) + \rho_g K_g \right\} \tag{3.42}$$

For a non-plug-in case, no electricity will be consumed on the ground. Therefore, eliminating the battery terms results in:

$$Emission = \left(1 - \frac{R \ - \frac{L}{D}\beta\left[\eta_{b\to p}\eta_{ch}\rho_g\alpha + (1-\alpha)\eta_{g\to p}\rho_g\right]}{\frac{L}{D}\beta\left[\eta_{b\to p}\left(\rho_b - \eta_{ch}\rho_g\alpha\right) - (1-\alpha)\eta_{g\to p}\rho_g\right]} \right) \beta W \rho_g K_g \tag{3.43}$$

The resulting optimal emission for a given desired range is shown in Figure 3.13.
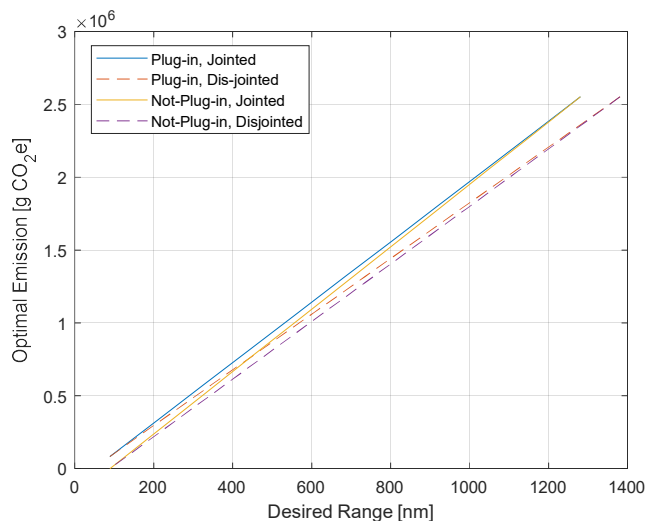
Figure 3.13. Optimal Emission vs. Desired Range.

$(W = 5{,}000 \; lbs., \beta = 0.3, \alpha = 0.5 \text{ for jointed})$

Similar to the optimal cost, the optimal emission increases linearly with range. This is reasonable since the further the aircraft travels, the more energy it consumes, which leads to more carbon emissions. Finally, the emission per distance travelled is plotted in Figure 3.14.
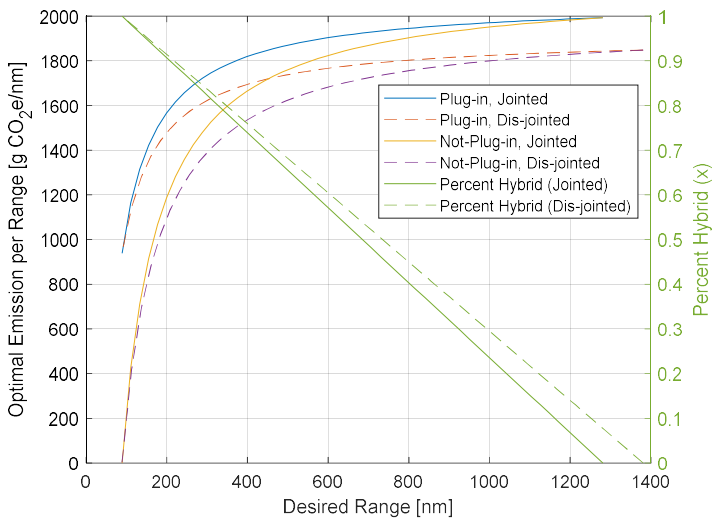
Figure 3.14. Optimal Emission per Range vs. Desired Range.

$(W = 5{,}000 \; lbs., \beta = 0.3, \alpha = 0.5 \text{ for jointed})$

Figure 3.14 shows that the non-plug-in case has lower emissions than the plug-in cases throughout until they converge at 100% hybrid, or a fully gas-powered system. This is due to the initial subtraction in emissions since no electricity is used to charge the battery. The fully electric non-plug-in cases are not practical options since there are no energy onboard at all. They are only shown to show the decreasing trend towards a fully electric hybrid system.

3.6.2. Total Emission

Since the number of cycles a battery can undergo before requiring replacement depends heavily on the design of the battery packs and their charge-discharge cycle, it is challenging to compute the exact total emissions without performing a lithium ion battery lifecycle analysis.

Another simpler approach is to assume an emission multiplier that depends on the battery capacity similar to that presented in Figure 2.11. If such emission value is known, an additional term can be added to Equation (3.40) to account for the emissions in battery manufacturing as shown:

$$Emission = (x\beta W \rho_{batt})\left(C_{batt} + \frac{C_{batt,prod}}{\# Cycle}\right) + [(1-x)\beta W \rho_{gas}]C_{gas} \qquad (3.44)$$

where $C_{batt,prod}$ would be the value shown in Figure 2.11, and '$\# Cycle$' is the number of cycles the battery can be used before needing replacement. Therefore, with increasing number of cycles, the impact of manufacturing will be smaller. Compared that to the emissions due to charging the battery, it is estimated that if the battery is used more than 20 times in its life, consuming gasoline will still produce more carbon emissions overall. Therefore, assuming an average battery will be operated for more than 20 fully discharge cycles before replacement, the optimal total emissions will still be when percent hybrid is

maximized.

3.7. Operational Objectives Considerations

In most design cases, there is a constraint on the size of battery that can limit the range

of percent hybrid. Two examples of such cases are emergency battery, and battery used

for flight control. In both cases, there is a specific power requirement that the battery

needs to satisfy. Based on a study on sizing battery packs for propulsive purposes (Zhao,

2018), it can be shown that the battery pack's configuration must satisfy the following set

of equations:

$$N_s = \left\lceil \frac{V_{motor}}{V_{cell}} \right\rceil$$

$$N_p = \left\lceil \frac{P}{V_{min}\, \eta_{motor}\, N_s\, Q_{cell}\, C_{max}} \right\rceil$$

(3.45)

Where N_s and N_p are the numbers of battery cells in series and parallel respectively.

Additionally, in the example of the emergency battery, there is also a requirement on the

duration the battery needs to supply the specified power. Therefore, an addition set of

equations must also be satisfied:

$$N_s = \left\lceil \frac{V_{motor}}{V_{cell}} \right\rceil$$

$$N_p = \left\lceil \frac{P \cdot t}{Q_{cell}\, V_{nom}\, \eta_{motor}\, N_s} \right\rceil$$

(3.46)

Since both Equations (3.45) and (3.46) need to be satisfied simultaneously for a

battery pack with both a power and endurance requirement, the number of cells in

parallel should be the higher of the two in order to provide enough electrical current for

the worst case load scenario. With the number of cells calculated, it is recommended to

verify if the resulting number of battery cells will provide enough power and energy, and

adjust as necessary.

The weight of the battery pack is the number of cells multiplied by the weight of one cell:

$$W_{batt} = \frac{N_s \, N_p \, W_{cell}}{W_c} \tag{3.47}$$

A knocked down value (W_c) is also added to account for the weight of the battery management system, cooling solution, and any items required to assemble the battery pack. This value is computed to be approximately 0.58 for the HK-36 electric airplane that weigh approximately 1,700 lb (Lilly, 2017), but is ultimately largely dependent on the specific design of the battery pack and the aircraft.

With the minimum number of cells and weight of the battery computed, the percent hybrid then must satisfy the following equation

$$x \geq \frac{W_{batt}}{W_{energy}} = \frac{N_s \, N_p \, W_{cell}}{W_c \beta W} \tag{3.48}$$

Therefore, for objectives where minimizing the weight of battery is optimal, the minimal value is governed by Equation (3.48).

Lastly, it must be noted that these equations listed are simply the first order approximation in sizing the battery pack. Other requirements such as multiple discharges and minimal cycle life will impose more equation requirements.

3.8. Jointed Operations

Jointed operation is characterized by the charging fuel weight fraction so far in this study. It is a parameter to describe how much fuel is used for charging the battery versus for propulsion. Therefore, it is possible to calculate the charging fuel weight fraction given a power profile. Assume the following profile shown in Figure 3.15, where the

battery is fully charged and discharged for the same amount of time continuously

throughout the mission.
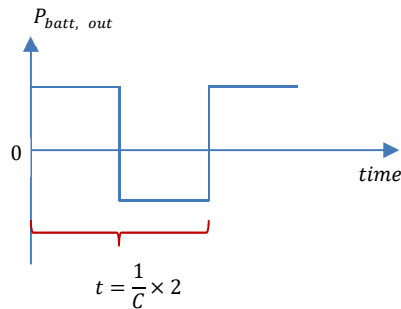
Figure 3.15. Example power profile.

A positive power means that the battery is providing power, whereas a negative value

means that it is being charged. Using a predetermined C-rate, the number of charge-

discharge (C-D) cycle for the mission can be found:

$$N_{CD\ cycles} = \left\lceil \frac{endurance}{2/C} \right\rceil \tag{3.49}$$

This number is rounded up to account for cases when the endurance is not integer

multiples of C-D cycle time. Next, the energy required to charge from the gas would then

be the energy capacity of the battery pack times the number of C-D cycle:

$$E_{gas}\ \eta_{charge} = E_{batt}N_{CD} \tag{3.50}$$

The energy of the battery pack can be expressed in terms of the motor voltage and battery

cell capacitance:

$$E_{batt} = V_{motor}Q_{cell}N_sN_p \tag{3.51}$$

and the energy of the gas can be expressed as the weight times the specific energy.

Substituting both into Equation (3.50) gives:

$$\left(W_{gas,ch}\rho_g\right)\eta_{ch} = \left(V_{motor}Q_{cell}N_sN_p\right)N_{CD} \tag{3.52}$$

Express the weight of gas used for charging in terms of the charging fuel weight fraction

gives:

$$\alpha W_{gas} \rho_g \eta_{ch} = V_{motor} Q_{cell} N_s N_p N_{CD} \tag{3.53}$$

Finally, substitute in Equation (3.7) for the weight of gas and solve for α in Equation (3.53):

$$\alpha = \frac{V_{motor} Q_{cell} N_s N_p N_{CD}}{(1-x)\beta W \rho_g \eta_{ch}} \tag{3.54}$$

This expression can be used if the power profile matches that shown in Figure 3.15. For a different power profile, a different method of finding the C-D cycle would be required. The charging fuel weight fraction can be iterated for optimal percent hybrid and energy weight fraction as necessary.

3.8.1. Range (Jointed)

The impact of the charging fuel weight fraction on range can be visualized using Equation (3.31). It is plotted at varying percent hybrid and charging fuel weight fraction at a constant energy weight fraction in Figure 3.16.
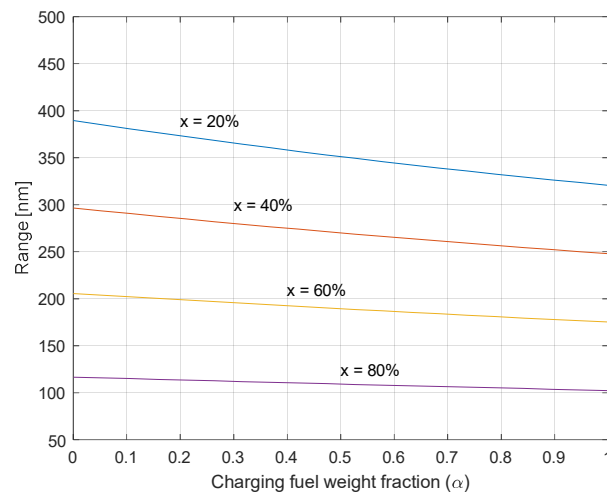
Figure 3.16. Range vs. charging fuel weight fraction at varying percent hybrid.

As shown in Figure 3.16 by the downward sloping curve as α increases, maximum range is achieved via minimizing charging fuel weight fraction no matter the percent hybrid. This is simply due to utilizing the gasoline to charge the battery at any capacity incurs additional loss in the energy conversion process. Therefore, for maximum range, it is preferable to maximize charging fuel weight fraction.

3.8.2. Cost and Emission (Jointed)

Jointed operation does not have a direct impact on cost and emissions for a constant weight and energy weight fraction formulation. This can be shown by the lack of charging fuel weight fraction in Equation (3.36) and (3.40). However, a jointed operation will increase the cost and emissions when a minimum range requirement is presented. The impact of which can be seen in Figure 3.10 and Figure 3.13 shown in the previous cost and emission sections.

4. Result and Analysis

The optimization results from the methodology section can be categorized into two cases – with and without a minimum range requirement. Without a minimum range requirement, in most cases, the optimal percent hybrid yields an integer solution, either 0 or 1. A summary of which is shown in Table 4.1 for all the design objectives discussed.

Table 4.1.

Optimal percent hybrid summary (without range requirement)

Optimize	Plug-in		Not plug-in	
	Jointed	Disjointed	Jointed	Disjointed
Weight	0	0	0	0
Weight (Peaks-and-Valleys)	Eq. (3.5)	-	-	-
Range	0	0	0	0
Operating Cost	1	1	1	1
Emission	1	1	1	1

With a minimum range requirement, however, there exists a non-integer solution for the design objectives that are optimum when percent hybrid is maximized. The percent hybrid for these cases are computed using Equation (3.35), reproduced here for reference:

$$x = \frac{R - \frac{L}{D}\beta[\alpha\eta_{g \to p}\rho_g - \eta_{b \to p}\eta_{ch}\rho_g(\alpha - 1)]}{\frac{L}{D}\beta\{\eta_{b \to p}[\rho_b + \eta_{ch}\rho_g(\alpha - 1)] - \alpha\eta_{g \to p}\rho_g\}} \tag{3.35}$$

Table 4.2 shows a summary of the reference equation for computing the optimal objective value with minimum range requirement.

Table 4.2.

Optimal percent hybrid summary (with range requirement)

	Plug-in		Not plug-in	
Optimize	Jointed	Disjointed	Jointed	Disjointed
Weight	0	0	0	0
Weight (Peaks-and-Valleys)	Eq. (3.5)	-	-	-
Operating Cost	Eq. (3.38)	Eq. (3.38) $(\alpha = 0)$	Eq. (3.39)	Eq. (3.39) $(\alpha = 0)$
Emission	Eq. (3.42)	Eq. (3.42) $(\alpha = 0)$	Eq. (3.43)	Eq. (3.43) $(\alpha = 0)$

Using this result, it is possible to determine a battery weight that will satisfy a range requirement and optimize the desired objectives. An example calculation is done in the following section to demonstrate the optimization process.

4.1. Application

A fictitious aircraft with properties listed in Table 4.3 will be used for the following calculations. The aircraft is modeled such that it has similar aerodynamics as a multi-copter since it is the expected airframe for serial hybrid architecture application. Namely, the aircraft will have a low lift-to-drag ratio. In addition to the variables shown, the efficiency values shown in Table 3.1 will also be used.

Table 4.3.

Properties of example aircraft

Parameter	Symbol	Value	Unit
Aircraft weight	W	5,000	lbs.
Energy Weight Fraction	β	0.3	-
Charging fuel weight fraction	α	0	-
Lift-to-Drag ratio	L/D	10	-
Average Power	P_{avg}	200	HP
Endurance	t	2	Hours

Table 4.3 (Cont'd)

Properties of example aircraft

Parameter	Symbol	Value	Unit
Motor Voltage	V_{motor}	400	V
Battery Knockdown value	W_c	0.5	-
Cell Capacitance	Q_{cell}	3.3	Ah
Nominal Cell Voltage	V_{cell}	3.6	V
Minimum Cell Voltage	V_{min}	2.5	V
C-rate discharge	C_{dis}	1	C
Cell Battery Weight	W_{cell}	0.1	lbs.

Next, identify all the constraints on the aircraft designs. These are objectives that must be satisfied. For this example, there will be two design constraints:

1. Range must be greater than 500 nautical miles

2. Battery must be sized to deliver an emergency power of at least 50 HP for 5 minutes

Under these two constraints, it is desired to compute the optimal percent hybrids for minimizing the direct operating cost.

4.2. Constraints

Since the constraints will impose a limit on the permissible range of percent hybrid, it is necessary to compute the corresponding limits first.

For the range constraint, Equation (3.35) can be used. To compute the percent hybrid, simply substitute in the 500 nm requirement as shown:

$$x = \frac{500\ nm - \frac{L}{D}\beta[\eta_{b\to p}\eta_{ch}\rho_g\alpha + (1-\alpha)\eta_{g\to p}\rho_g]}{\frac{L}{D}\beta[\eta_{b\to p}(\rho_b - \eta_{ch}\rho_g\alpha) - (1-\alpha)\eta_{g\to p}\rho_g]} = 0.68 \qquad (4.1)$$

Using the aircraft properties listed, Equation (4.1) results in a percent hybrid of

approximately 68%. Recall that maximum range occurs when percent hybrid is minimized. Therefore, the computed value is the maximum allowable percent hybrid. Beyond this, the aircraft will not be able to achieve a 500 nm range.

The second requirement on battery sizing is an operational constraint. Since both power and endurance requirements are specified. The battery must be sized for both requirements and the larger of the two will be used. For the power requirement, Equation (3.45) will be used to compute the number of battery cells:

$$N_s = \left\lceil \frac{V_{motor}}{V_{cell}} \right\rceil = 112$$

$$N_p = \left\lceil \frac{50\ HP}{V_{min}\ \eta_{EM}\ N_s\ Q_{cell}\ C_{dis}} \right\rceil = 45$$

(4.2)

Caution that the appropriate unit conversion should be used in the above equations to obtain the proper value. For the endurance requirement, Equation (3.46) will be used:

$$N_s = \left\lceil \frac{V_{motor}}{V_{cell}} \right\rceil = 112$$

$$N_p = \left\lceil \frac{50\ HP \cdot 2\ hours}{Q_{cell}\ V_{nom}\ \eta_{EM} N_s} \right\rceil = 3$$

(4.3)

Since the number of cells in parallel is greater when sizing for the power requirement, using that will also satisfy the endurance requirement. Therefore, the weight of the battery pack can be computed using Equation (3.47):

$$W_{batt} = \frac{112 \cdot 45 \cdot W_{cell}}{W_c} = 888\ lbs$$

(4.4)

Finally, given the battery weight, it is then possible to compute the corresponding percent hybrid:

$$x = \frac{888\ lbs}{\beta W} = 0.59$$

(4.5)

Since the specified emergency power and endurance are minimum requirements, the percent hybrid must be greater than 59% to satisfy the constraints.

Using these two constraints, both upper and lower bounds on percent hybrid are obtained, and a summary is shown in Table 4.4 below.

Table 4.4.

Constraints on Percent Hybrid

#	Constraint	Percent Hybrid Limit
1	Range > 500 nm	$x < 68\%$
2	Emergency 50 HP for 5 mins	$x > 59\%$

4.3.   Objective Optimization

All the objectives discussed in this study can be optimized by maximizing or minimizing percent hybrid. Therefore, the optimal percent hybrid for minimizing operating cost will be either at 59% or 68%. To determine the optimal percent hybrid, simply refer to Table 4.1.

Under direct operating cost, the optimal percent hybrid is one, or 100%. So, 68% hybrid will yield the optimal cost for this example. Using Equation (3.36) with the energy cost shown in Table 2.3, the optimal operating cost is:

$$Cost = \mathbf{0.68}\beta W \rho_{batt} C_{batt} + (1 - \mathbf{0.68})\beta W \rho_{gas} C_{gas} = \$135 \qquad (4.6)$$

The cost shown in Equation (4.6) is the minimum direct operating cost associated with the constraints set forth in this example. A different percent hybrid between 59% and 68% will yield a higher cost but still satisfy the constraints. Table 4.5 shows a comparison in cost if the minimum permissible percent hybrid is chosen instead.

Table 4.5.

Comparison between minimum and maximum percent hybrid

Objectives	Description	$x = 59\%$	$x = 68\%$
Constraint 1	Range >500 nm	949 nm	500 nm
Constraint 2	Emergency 50 HP for 5 mins	50 HP for 5 mins	85 HP for 5 mins
Optimize	Cost	$237	$135

Using the lowest percent hybrid in the permissible range yields approximately a 75%

increase in direct operating cost. However, due to the decrease in percent hybrid, the

range has almost doubled that specified in the design constraints. Therefore, the user has

the flexibility to adjust the percent hybrid within this range to see the tradeoff between

constraints and optimization objectives.

5. Conclusion

5.1. Significant Results

Battery weight in hybrid aircraft has a significant impact on the performance of the aircraft. By simply varying the ratio between battery weight and fuel weight, it is possible to drastically change the outcome of different design objectives.

In general, if there are no constraints on the aircraft design, the optimal percent hybrid yields a simple integer solution. This means that either a conventional gas engine or an electric motor will likely to provide the best result. However, if there are one or more constraints, they introduce boundaries for the range of permissible percent hybrid. In such cases, the optimal percent hybrid will become a non-integer solution that depends on the type of constraints applied.

In this study, a special focus is placed on the minimum range constraint due to its popularity in aircraft design. It is shown that there is a maximum allowed percent hybrid for any reasonable range requirement. Such percent hybrid could then be used to find the optimal operating cost and carbon emissions, which are two of the considered objectives. Since it only imposes an upper percent hybrid boundary, any percent hybrid smaller than that will also satisfy the range requirement. Therefore, the aircraft designers can also use the above relationship to evaluate the tradeoff between range, weight, cost, and emissions for their specific aircraft.

Additionally, using the assumed serial hybrid architecture, it is found that a jointed operation between the gas engine and electric motor will likely reduce the overall performance of the aircraft. Notably, the range will decrease whenever gasoline is used to charge the battery due to losses in storing and extracting energy from the battery.

5.2.   Future Work

Battery charge and discharge characteristics are dynamic and dependent on the type of battery used. For most of the derivations presented, it is assumed that all the energy in the battery can be used, and it can be charged to its maximum advertised capacity. Though a constant efficiency term is added to account for the loss, this assumption neglected the dynamic aspect of power delivery from the battery, such as the decrease in voltage at different states of charge. Therefore, it is recommended that additional battery testing be performed to understand the amount of energy or power that can be discharged. Doing so will improve the fidelity of the derived relationships and can provide a more practical and accurate percent hybrid estimation.

For cost and emissions, a more elaborate study on the life cycle analysis of Li-ion battery could prove beneficial for understanding the overall emissions and cost of the mission. Due to the numerous variables that can impact the outcome of a battery's life cycle, the total cost analysis was left out in this study. As more research surfaces on the public domain, or through personal battery testing, the total life cycle analysis should be incorporated to see if there are any changes in trend for overall cost and emissions.

REFERENCES

Air British Petroleum. (2000). Handbook of Products [PDF file].

Argonne National Laboratory (2012). Carbon Trip Calculator. Retrieved from https://greet.es.anl.gov/trip-calculator

Argonne National Laboratory (n.d.). GREET ® Model. Retrieved from https://greet.es.anl.gov/index.php

Argonne National Laboratory (2018). The Greenhouse Gases, Regulated Emissions, and Energy Use in Transportation (GREET) Model [Computer Software]. Available from https://greet.es.anl.gov/index.php

Eckert, J. J., Corrêa, F. C., Santiciolli, F. M., Costa, E. D., Dionísio, H. J., & Dedini, F. G. (2015). An Influence Study Of Parallel Hybrid Vehicle Propulsion System Configurations. *Anais Do XXIII Simpósio Internacional De Engenharia Automotiva*. doi:10.5151/engpro-simea2015-pap130

Emadi, A., Lee, Y., & Rajashekara, K. (2008). Power Electronics and Motor Drives in Electric, Hybrid Electric, and Plug-In Hybrid Electric Vehicles. *IEEE Transactions on Industrial Electronics, 55*(6), 2237-2245. doi:10.1109/tie.2008.922768

Gartenberg, L. (2017). *Battery Centric Serial Hybrid Aircraft Performance and Design Space*. Embry-Riddle Aeronautical University.

Hall, D., & Lutsey, N. (2018). Effects of battery manufacturing on electric vehicle life-cycle greenhouse gas emissions. The International Council on Clean Transportation.

Hao, H., Mu, Z., Jiang, S., Liu, Z., & Zhao, F. (2017). GHG Emissions from the Production of Lithium-Ion Batteries for Electric Vehicles in China. *Sustainability, 9*(4), 504. doi:10.3390/su9040504

Hepperle, M. (2012). Electric Flight - Potential and Limitations. *German Aerospace Center*.

Kessler, R. (2013). Sunset for Leaded Aviation Gasoline? *Environmental Health Perspectives, 121*(2). doi:10.1289/ehp.121-a54

Kim, H.D. (2010). Distributed Propulsion Vehicles. *International council of aeronautical sciences*

Kokam. (n.d.). Superior Lithium Polymer Battery (SLPB) KOKAM Li-ion/Polymer Cell [PDF file]. Retrieved from http://kokam.com/data/Kokam_Cell_Brochure_V.1.pdf

Lilly, J. (2017). *Aviation Propulsive Lithium-Ion Battery Packs State-of-Charge and state-of-Health Estimations and Propulsive Battery System Weight Analysis*. Embry-Riddle Aeronautical University.

Lyasoff, R. (2016, September 23). Welcome to Vahana [Web log post]. Retrieved from https://vahana.aero/welcome-to-vahana-edfa689f2b75

Marwa, M., Martos, B., Martin, S. M., & Anderson, R. (2017). Analytical Forms of the Range Performance of Hybrid and Electric Turboprop Aircraft, for Design Optimization Studies. *55th AIAA Aerospace Sciences Meeting*. doi:10.2514/6.2017-0211

Panasonic. (2012). Lithium Ion NCR18650B [PDF file]. Retrieved from https://www.batteryspace.com/prod-specs/NCR18650B.pdf

Raley, D (2018). Seeing beyond the horizon. *Innovation Quarterly, Boeing Worldwide*. Retrieved from http://www.boeing.com/features/innovation-quarterly/feb2018/feature-horizon.page

Reddy, T. B., & Linden, D. (2011). *Lindens handbook of batteries*. New York: McGraw-Hill.

Rosales, J. M., & Anderson, R. (2019). Gas-Battery vs. Gas-Only Serial Hybrid Propulsion System Comparison. *AIAA Scitech 2019 Forum*. doi:10.2514/6.2019-1673

Storm, R., Skor, M., Koch, L., Benson, T., & Galica, C. (2007). *Pushing the envelope: A NASA guide to engines*. Washington, DC: National Aeronautics and Space Administration, John H. Glenn Research Centers Educational Programs Office.

Uber Technologies Inc. (2016). Fast-Forwarding to a Future of On-Demand Urban Air Transportation. Retrieved from https://www.uber.com/elevate.pdf/

United States Energy Information Administration. (2019). *Annual Energy Outlook 2019, Table: Energy Prices by Sector and Source*. Retrieved from https://www.eia.gov/outlooks/aeo/data/browser/#/?id=3-AEO2019&sourcekey=0

Vertical Flight Society. (2019, April 16). EVTOL Aircraft Directory. Retrieved from http://evtol.news/aircraft/

Zhao, T. (2018). *Propulsive Battery Packs Sizing for Aviation Applications*. Embry-Riddle Aeronautical University.